

Design of All-Solid Bandgap Fiber With Improved Confinement and Bend Losses

Guobin Ren, Ping Shum, *Senior Member, IEEE*, Liren Zhang, Min Yan, Xia Yu, Weijun Tong, and Jie Luo

Abstract—We propose a new design of low-contrast all-solid bandgap fiber with low confinement and bend losses within low-order bandgaps. By introducing an index depressed layer around the high index rod in fiber cladding, we theoretically predict that the confinement loss of the proposed all-solid bandgap fiber would be significantly improved. Due to the enlarged index mismatch of the guided core mode and the edge of the bandgaps, the critical bend radius of the proposed fiber is remarkably reduced.

Index Terms—Bend loss, confinement loss, photonic bandgap, photonic crystal fiber.

I. INTRODUCTION

ALL-SOLID bandgap fiber is an optical fiber whose cladding consists of an array of isolated high index rods in a low index background material, the fiber core is generally a low index area formed by omitting one or several rods [1]–[3]. The antiresonant reflection optical waveguide model [4], [5] has been successfully applied to understand the guidance mechanism of all-solid bandgap fiber. Unlike solid core photonic crystal fibers with air inclusions, which have broadband transmission, these fibers have discrete bands of high transmission corresponding to the bandgap of the fiber cladding. Recently, all-solid bandgap fibers made from fused silica with refractive index contrast as low as 1% has been reported [2]. The low-contrast all-solid bandgap fibers provide a promising technology to fabricate bandgap materials with usual process used in conventional fiber drawing. Comparing to air-core bandgap fiber, all-solid bandgap fiber is better to realize rare-earth-doped amplifier and laser or to write Bragg gratings which are widely used in photonics. Furthermore, these fibers should be easier to fabricate and splice for its elimination of mechanically unstable holey structure.

At present, the lowest loss for such all-solid bandgap fibers is about 20 dB/km [6]. But almost all these fibers utilize the high-order bandgaps. Furthermore, these fibers have been found to suffer from significant bend loss under certain circumstances. Although high-order bandgaps provide lower confinement loss, they are more sensitive to fiber deformation, and the photonic

Manuscript received September 1, 2006. This work was supported in part by the project (M47040039) of the Agency for Science, Technology and Research, Singapore, and by the Open Fund of Key Laboratory of Optical Communication and Lightwave Technologies, (Beijing University of Posts and Telecommunications), Ministry of Education, China.

G. Ren, P. Shum, L. Zhang, M. Yan, and X. Yu are with the Network Technology Research Centre, Nanyang Technological University, Singapore 637553, Singapore.

W. Tong and J. Luo are with Yangtze Optical Fiber and Cable Co. Ltd., Wuhan 430073, China.

Color versions of Figs. 1, 2, 4, and 5 are available at <http://ieeexplore.ieee.org>. Digital Object Identifier 10.1109/LPT.2006.887227

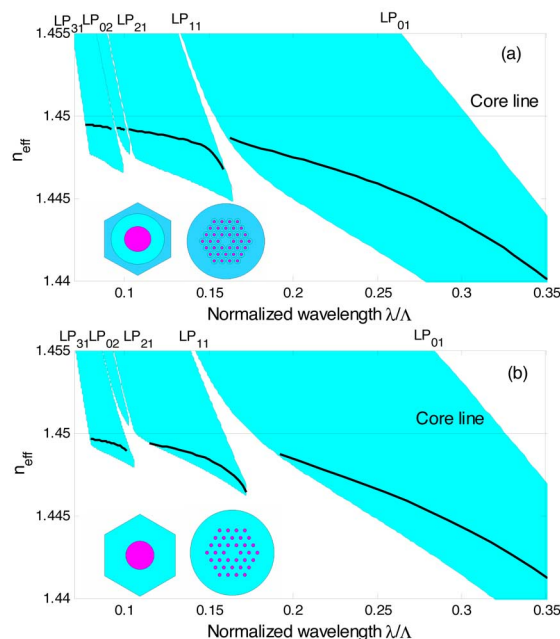


Fig. 1. (a) Bandgap map and guided modes of Fiber A. (b) Bandgap and guided modes of Fiber B. Only 1–4 bandgaps are shown in figure. The axes are effective indexes n_{eff} and normalized wavelength λ/Λ . At the top of each figure, LP_{ml} marked the photonic bands of cladding. The inset shows the unit cell and fiber profile of bandgap fiber.

bands of high-order rod modes will greatly narrow the transmission windows of the fiber. Furthermore, working in higher bandgaps at a fixed wavelength would require larger pitch and inturn thicker fibers. In this letter, we proposed a new design of low-contrast bandgap fiber with low confinement loss especially in low-order (first and second) bandgaps. The critical bend radius analysis shows the proposed fiber is more resistant to bend loss.

II. CONFINEMENT LOSS

The plane-wave method and finite-difference method (FDM) with PML boundary [6] are used to calculate the photonic bandgap map and guided modes of all-solid bandgap fibers, respectively.

The proposed low index contrast bandgap fibers have a triangular lattice of rods in cladding; the fiber core is formed by omission of one rod. The unit cell of the cladding and fiber profile are shown in the inset of Fig. 1(a). The unit cell composed of a high index rod (with diameter $d_h = 0.4\Lambda$, Λ is the lattice spacing) surrounded by an index depressed layer (with diameter $d_l = 0.8\Lambda$). The background silica index n_m is assumed to be 1.45, the index of the rod and the depressed outer layer is set as $n_h = 1.4858$ and $n_l = 1.4428$, respectively,

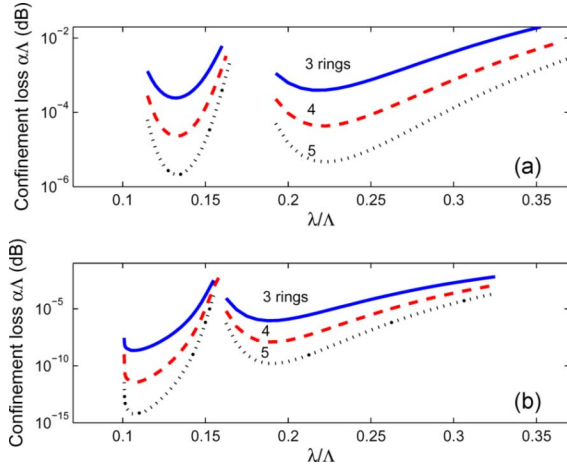


Fig. 2. Confinement losses as a function of normalized wavelength λ/Λ and the number of the rings of rods in cladding within first and second bandgaps. (a) Fiber B; (b) Fiber A.

which correspond to germanium-doped silica $\Delta_h = 2.5\%$ and fluorine-doped silica $\Delta_l = -0.5\%$. For simplicity, it is called Fiber A.

In Fig. 1(a), we show the bandgap map and guided core mode of all-solid bandgap Fiber A. The photonic bands formed by the coupling of the modes of isolated high index rods are marked at the top of the map. The core line $n_{\text{eff}} = 1.45$ represents the boundary between states that are propagating or evanescent in background material of cladding. Since we focus on the modes in low-order (first and second) bandgap, only one to four bandgaps are shown in figure. Note that the low-order bandgaps are much wider and more deformation-resistant than high-order ones [3]; therefore, it is desirable to operate a fiber in these bandgaps.

For comparison, we calculated a bandgap fiber (called Fiber B) with similar configuration to Fiber A. The only difference is that we removed the index depressed layer in the unit cell of the fiber cladding. Fig. 1(b) shows the bandgap map and guided modes of Fiber B. By comparing Fig. 1(a) with (b), we noticed that the bandgaps shift to the blue edge of the spectrum when an index depressed layer is introduced. Furthermore, the bandgaps of Fiber A exhibit much deeper floors than those of Fiber B.

The confinement losses of Fibers A and B with different numbers of rings of rods in cladding are shown in Fig. 2. The confinement losses are normalized to $\alpha\Lambda$ (in decibels), but may be scaled for any chosen value of the lattice spacing. It is evidently that the high-order bandgap provides lower confinement loss than low-order ones, and the increase of number of rings efficiently decreases the confinement loss. We noticed the confinement loss is relatively high in first and second bandgaps for Fiber B, even if five rings of rods are included in the cladding. For the first bandgap, the minimum normalized confinement loss is about $4.6 \cdot 10^{-6}$ dB at $\lambda/\Lambda = 0.22$, while for the second bandgap, is about $2.1 \cdot 10^{-6}$ dB at $\lambda/\Lambda = 0.133$. Although the confinement loss can be reduced simply by increasing the number of the rings, this will result in a thicker fiber diameter (generally exceeding $125 \mu\text{m}$).

The confinement loss is remarkably reduced in Fiber A. Although the bandgaps and the minimum wavelengths of

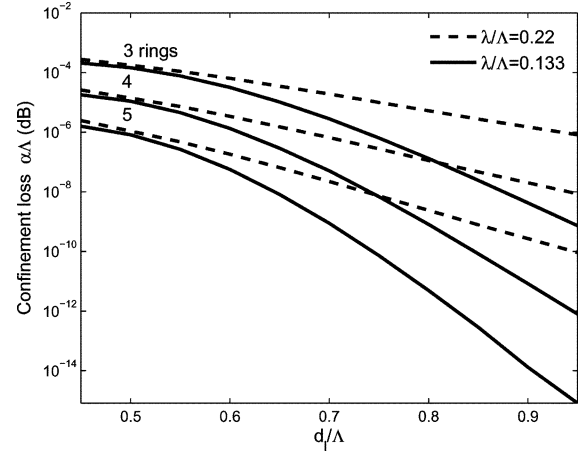


Fig. 3. Confinement loss versus d_l/Λ at two normalized wavelength $\lambda/\Lambda = 0.133$ and $\lambda/\Lambda = 0.22$ with three, four, five rings of rods in fiber cladding.

confinement loss shifted to the short wavelength direction, the confinement loss is about $2.4 \cdot 10^{-9}$ dB at $\lambda/\Lambda = 0.22$, and $4.96 \cdot 10^{-12}$ dB at $\lambda/\Lambda = 0.133$ for Fiber A with five rings of rods in cladding.

It is confirmed that the bandgap map would shift to the blue edge of the spectrum when the diameter of the index depressed layer (d_l) increases. Although the minimum confinement loss may not keep at a fixed wavelength, we show the effect of the index depressed layer on confinement loss at two normalized wavelengths $\lambda/\Lambda = 0.133$ and $\lambda/\Lambda = 0.22$ in Fig. 3. It is shown that the confinement loss decreases monotonically as d_l increases. The confinement loss decreases more rapidly within the second bandgap than that of the first bandgap with increasing d_l .

The index depressed layer around the high index rods in cladding will reduce the confinement loss of the fiber, but they also introduce the possibility of guiding by total internal reflection (TIR). To investigate the guidance mechanism of the proposed fiber, we compared the proposed Fiber A with Fiber C, which has the same configuration as Fiber A except the high index rod in the unit cell is removed, and only the index depressed layer is left. In Fig. 4(a), we show a bandgap map, guided modes of Fiber A, and the guided mode of Fiber C. It is noticed that the guided mode of Fiber A only exists within the bandgap, while it is continuous for Fiber C. The modal dispersion of Fiber A is quite different from that of Fiber C, especially at the edge of the bandgap. In Fig. 4(b), we have shown the normalized effective areas A_{eff}/Λ^2 of guided modes for Fibers A and C. We see that the modal field of Fiber A is more confined than that of Fiber C, and the effective area difference increases with increasing wavelength within the bandgap. At $\lambda/\Lambda = 0.25$, the A_{eff} has a value of $1.43\Lambda^2$ (well confined mode) for Fiber A, while $A_{\text{eff}} = 3.9\Lambda^2$ (delocalized mode) for Fiber C. The reason for this observation is obvious: for Fiber A, the better confinement is due to the photonic bandgap effect provided by the high index rods (or along with the low index ring) in cladding. This analysis implied that the guided mechanism of the proposed fiber is partially involved TIR especially at short wavelength, however, it is mainly the photonic bandgap effect or antiresonant reflection at long wavelength region (low order bandgaps) which is our focus in this letter.

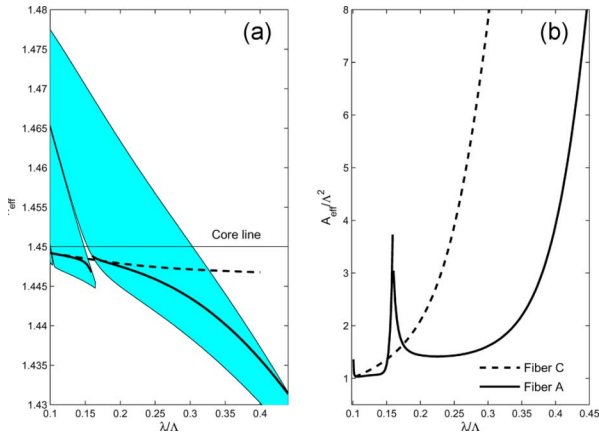


Fig. 4. (a) Bandgap map and guided modes of Fiber A, and the guided mode of Fiber C (dotted line). (b) Normalized effective areas of guided mode A_{eff}/A^2 as a function of normalized wavelength λ/A within first and second bandgaps for Fiber A and Fiber C.

III. BEND LOSS

In conventional step index fiber, bend loss arises from the resonant coupling of light from core to radiation modes in cladding on the outside of the bend. The refractive index profile of fiber increases linearly with distance on the outside of the bend; bend loss occurs centrifugally at a distance, where the cladding index is raised enough to match the effective index of core mode. The bend loss mechanism is similar for bandgap fibers, except that the photonic bands exist at higher as well as lower index than the core mode. The bend loss is mainly centrifugal near the blue edge of a bandgap, whereas is centripetal near the red edge of a bandgap [3].

In low-contrast bandgap fibers, the critical bend radius R_c below which bend loss becomes large is approximately [8]

$$R_c \approx \frac{4\pi\lambda n_m^2}{|n_{\text{fm}}^2 - n_{\text{edge}}^2|^{3/2}} \quad (1)$$

where n_m is the refractive index of background, n_{fm} is the effective index of fundamental mode, and n_{edge} is effective index of the edge of bandgaps.

Except the improved confinement loss, the fiber proposed here also shows decreasing bend sensitivity. Fig. 5 shows normalized critical bend radius R_c/Λ for first and second bandgaps. Fiber D is a fiber similar to Fiber A, except that the diameter of the index depressed layer is $d_l = 0.6\Lambda$. It is noticed that as the diameter of the index depressed layer increases, the bandgaps shift to the blue edge of the spectrum, and the critical bend radius is significantly reduced. The mode guided by the second bandgap is more susceptible for bend loss than that guided by first bandgap. Furthermore, the difference of susceptibility to bend loss in first and second bandgaps is relatively high for Fiber B.

The index depressed layer in unit cell of cladding provides more strong confinement, which helps LP_{lm} rod modes decay more quickly into background material. The rod modes, therefore, are more weakly coupled and the photonic bands are narrower. It is shown that the floor and the blue edge of a bandgap

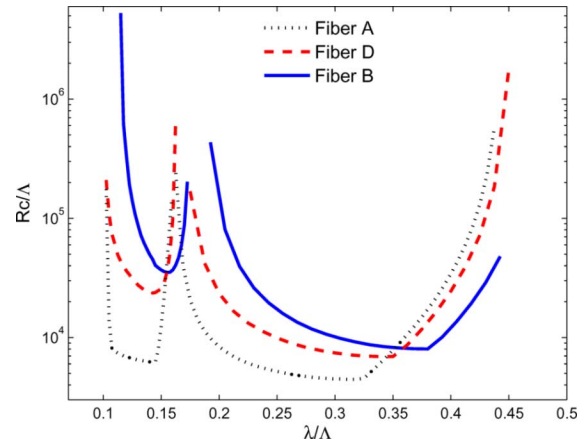


Fig. 5. Normalized critical bend radius R_c/Λ versus normalized wavelength λ/Λ of all-solid bandgap fibers within first and second bandgaps.

are defined by the same rod mode [8]. So the result is the floor and the blue edge of a bandgap are deepened eventually (see Fig. 1). The deepened floor of bandgap then increases the mismatch of effective index between guided core mode and the floor of bandgap. According to (1), the critical bend radius, therefore, decreases with increasing mismatch of refractive index.

IV. CONCLUSION

We have proposed a new design of low-contrast all-solid bandgap fiber. It is shown that the confinement loss of the proposed fiber is significantly reduced compared with all-solid bandgap fiber whose cladding consists of simple high index rods. The floor of the bandgaps is efficiently deepened by introducing an index depressed layer around the high index rods in the unit cell of photonic crystal cladding. Due to the enlarged index mismatch of the guided core mode and the edge of the bandgaps, the critical bend radius of the proposed fiber is remarkably reduced.

REFERENCES

- [1] F. Luan, A. K. George, T. D. Hedley, G. J. Pearce, D. M. Bird, J. C. Knight, and P. St. J. Russell, "All-solid photonic bandgap fiber," *Opt. Lett.*, vol. 29, pp. 2369–2371, 2004.
- [2] A. Argyros, T. A. Birks, S. G. Leon-Saval, C. M. B. Cordeiro, F. Luan, and P. St. J. Russell, "Photonic bandgap with an index step of one percent," *Opt. Express*, vol. 13, pp. 309–314, 2005.
- [3] A. Argyros, T. A. Birks, S. G. Leon-Saval, C. M. B. Cordeiro, and P. St. J. Russell, "Guidance properties of low-contrast photonic bandgap fibres," *Opt. Express*, vol. 13, pp. 2503–2511, 2005.
- [4] T. P. White, R. C. McPhedran, C. M. de Sterke, N. M. Litchinitser, and B. J. Eggleton, "Resonance and scattering in microstructured optical fibers," *Opt. Lett.*, vol. 27, pp. 1977–1979, 2002.
- [5] N. M. Litchinitser, S. C. Dunn, B. Usner, B. J. Eggleton, T. P. White, R. C. McPhedran, and C. M. de Sterke, "Resonances in microstructured optical waveguides," *Opt. Express*, vol. 11, pp. 1243–51, 2003.
- [6] G. Bouwmans, L. Bigot, Y. Quiquempois, F. Lopez, L. Provino, and M. Douay, "Fabrication and characterization of an all-solid 2-D photonic bandgap fiber with a low-loss region (< 20 dB/km) around 1550 nm," *Opt. Express*, vol. 13, pp. 8452–8459, 2005.
- [7] S. Guo, F. Wu, S. Albin, H. Tai, and R. S. Rogowski, "Loss and dispersion analysis of microstructured fibers by finite-difference method," *Opt. Express*, vol. 12, pp. 3341–3352, 2004.
- [8] T. A. Birks, F. Luan, G. J. Pearce, A. Wang, J. C. Knight, and D. M. Bird, "Bend loss in all-solid bandgap fibres," *Opt. Express*, vol. 14, p. 5688, 2006.